Investigating the Observability of Monocular SLAM: Obscured Beacons and Disparity Measurements

Talha Manzoor[1] and Abubakr Muhammad[1]

Department of Electrical Engineering
LUMS School of Science and Engineering
Lahore, Pakistan

Abstract. In this paper we concern ourselves with the observability of monocular SLAM from a non-linear control theory perspective. Such a study is necessary for a full understanding of the monocular SLAM problem and helps formulate the necessary conditions to make it converge. Past work has focused on using observability analysis performed on linearly approximated systems, to calculate the unobservable directions for incorporating into the robot motion planner. Here we focus on conditions to mantain observability at all times, keeping in view robotic applications with predetermined coverage strategies like mine-sweeping and surveillance robots. The observability analysis performed herein helps us to determine the number of known landmarks (beacons) necessary for SLAM convergence. We calculate observability while preserving the nonlinearity of the system, which also provides a comparison with the results obtained previously with linear techniques. We use this analysis to build a strategy for maintaing observability when the beacons are obscured from sight. We acheive this by considering the most certain landmark at the time of beacon obscurity, as a secondary beacon. This allows the rest of the states to continue to converge, and the price we pay is in form of the levelling off of the estimate of the "beaconized" landmark. We also provide an understanding of the need for triangulation for full state reconstruction by including disparity as a separate measurement. We then consider the effect of including disparity as a measurement in the Kalman filter and show that this will cause an increase in the measurement noise covariance before being incorporated into the filter. This is due to the fact that disparity is a measurement dependent on the current and previous states whereas the Kalman filter requires that the measurement be a function of the current state only. Where applicable, we reconcile our theoretical findings with numerical simulations and present the results.

1 Introduction

Simultaneous Localisation and Mapping with a single camera, also known as Monocular SLAM, is a well known problem in the robotics community and extensive research and development have been carried out in this area. One major concern while deploying a single camera as a sensor for any mapping problem is the inherent handicap in trying to reconstruct the environment from a single image. By construction, a single camera measurement only provides the bearing to a particular point and so, we are unable to extract any depth information from it. This leads one to wonder about the extent to which

Monocular SLAM may or may not work. To date, many such systems have been developed and successfully implemented, which proves empirically that the SLAM process while using a single camera does indeed converge. A rigorous analytical proof however, can be provided by the observability of non-linear systems as studied in control theory.

The observability of monocular (or bearing-only) SLAM has been investigated in the past as well. Bonnifait and Garcia [1] carry out an observability analysis of a planar robot trying to localise itself, given the bearing to 3 known beacons. They use tools from non-linear observability theory and conclude that the system is observable except for the degenerate case when the robot is located on the circle defined by the 3 beacons and is stationary. They also consider the affect on system observability when one or more of the beacons are obscured from sight.

In a similar paper, Calleja et al [2] have considered the observability of a planar robot, performing SLAM with a bearing-only sensor. Instead of expressing the SLAM system in its regular form, they do so in the error form presented in [3]. This allows them to approximate the system as piecewise constant, enabling them to use linear observability techniques as given in [4]. This greatly reduces the complexity of the analysis. Furthermore this approach allows them to calculate a basis for the unobservable subspace, given by the null space of the stripped observability matrix. They suggest that such information may be integrated in the robot's motion planning algorithm so as to avoid the unobservable directions. They conclude that for absolute coordinates SLAM, the process is unobservable over 2 time segments when the robot is either stationary, or moving directly towards a landmark. Introducing a known landmark (beacon) renders the linearly approximated process fully observable.

Tribou et al [5] present an observability analysis for a planar position based visual servoing system, also applicable to monocular SLAM. They focus on determining the unobservable configurations for their application. They too approximate the system with a piecewise constant one and the analysis is similar to that of [2]. However, instead of a specific kinematic model for the vehicle, they consider a constant velocity motion model which constitutes a larger unobservable subspace then the vehicle specific kinematic model. They consider cases both where target feature points are known and unknown prior to the estimation process.

The previous work mentioned here focuses on using observability analysis to determine the unobservable directions, for the robot to avoid for better state estimation. However, the liberty to follow such directions may not exist for robots in applications like landmine clearance and surveillance, where it is extremely essential that the robots follow a predetermined coverage strategy over the field, as presented in [6]. Such a situation may also arise by constraints imposed by the terrain for outdoor robots or by the structure of the environment for indoor robots. We instead, focus on using observability analysis to determine the number of beacons (known landmarks) required to mantain observability of monocular SLAM at all times. Our motivation stems from the single camera SLAM system first presented by Davison [7], in which the SLAM process is initialized with a certain number of known landmarks. This empirically suggests that in order to prevent the error to drift, it is necessary to place beacons in the environment.

Although, Calleja et al [2] have determined that 1 beacon and 2 time segments is sufficient to guarantee observability, we also provide a strategy on how to maintain

observability when the beacon is obscured from the robot. We do this, by eliminating one or more estimated landmarks from the state vector, thus treating it as a beacon. We discuss how to determine which landmarks qualify for this "beaconization" at any point in time, and what effect this would have on the measurement noise. We also discuss the theoretical bound after which it would be necessary to re-observe the original beacon, a process similar to the regular resurfacing of a sea diver for a breath of air, in order to keep himself from drowning.

Another contribution of this work is that we carry out a non-linear analysis as presented by Hermann and Krenner [8] instead of the linearised approximation. This enables us to consider the SLAM system in its regular form, which is more expressive as opposed to the linearised error form. The analysis is more complex and so, we have used a bottom up approach in which we start from the simplest case possible, a 1-D localising robot (the Monobot), and steadily build up towards the general non-linear planar case by adding DOF's at each step. Towards the end, the analysis becomes extremely complex, so much so that it becomes practically unsolvable even by a computer algebraic package. In this case, we are able to provide a geometrical argument, an approach also followed in [1].

We also formalize the notion of the need for triangulation in order to fully reconstruct the state. In [2], this formalization has been done by considering observability over multiple time segments. We in turn, are using non-linear tools and are concerned with instantaneous observability. We have thus calculated the observability while incorporating disparity as a separate measurement. We then consider the effect of disparity as a measurement in the Kalman filter, as disparity is a measurement dependent on the current and previous states, whereas the measurement model of the Kalman filter represents its relationship with the current state only.

2 Observability Analysis for the Monobot

In this section we analyse the observability for the Monobot, a robot restricted to move on a single line with all landmarks situated at a known depth. We use a constant velocity motion model for all cases.

2.1 Case 1: 1-DSLAM

Consider the robot to be constrained to move on a single line, and observing a single landmark to estimate its position and the location of the landmark (Figure 1).

The state vector will be given by

$$X_k = \begin{bmatrix} c_k \\ \dot{c}_k \\ x_{L1_k} \end{bmatrix} \tag{1}$$

where c_k and $\dot{c}_k$ are the robot position and velocity respectively, and x_{L1_k} is the location of the landmark $L1$. The constant velocity process model will be given as

$$F = \begin{bmatrix} 1 & \Delta t & 0 \\ 0 & 1 & 0 \\ 0 & 0 & 1 \end{bmatrix} \tag{2}$$

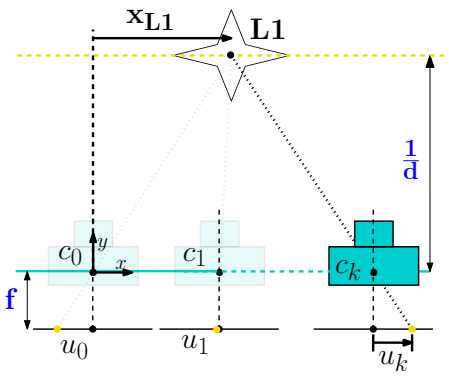

Fig. 1. The monobot performing SLAM with 1 landmark. The focal length of the camera is given by f and the inverse depth of the landmark is given by d.

The measurement equation can be found through similar triangles to be

$$h_{k+1} = u_{k+1} = x_{L1_{k+1}} fd - c_{k+1} fd \tag{3}$$

And so the measurement matrix will be

$$H = [-fd \quad 0 \quad fd] \tag{4}$$

As the system is linear, the observability matrix will be given as in [9], by

$$O = \begin{bmatrix} H \\ HF \\ HF^2 \end{bmatrix} = \begin{bmatrix} -fd & 0 & fd \\ -fd & -\Delta t fd & fd \\ -fd & -2\Delta t fd & fd \end{bmatrix} \tag{5}$$

We see that the observability matrix does not have full rank and hence the process is unobservable.

2.2 Case 2: SLAM with 1 Beacon

Robot contrained to move on a line, observing a beacon and a single unknown landmark, to estimate the position of itself and the unknown landmark (Figure 2).

The state vector will become

$$X_k = \begin{bmatrix} c_k \\ \dot{c}_k \\ x_{L2_k} \end{bmatrix} \tag{6}$$

The matrix F for the process model will be the same as that given in Equation 2. As x_{L1} is now known, the measurement equations will be given by

$$h_{1_{k+1}} = u1_{k+1} - x_{L1} fd = -c_{k+1} fd \tag{7}$$

$$h_{2_{k+1}} = u2_{k+1} = x_{L2_{k+1}} fd - c_{k+1} fd \tag{8}$$

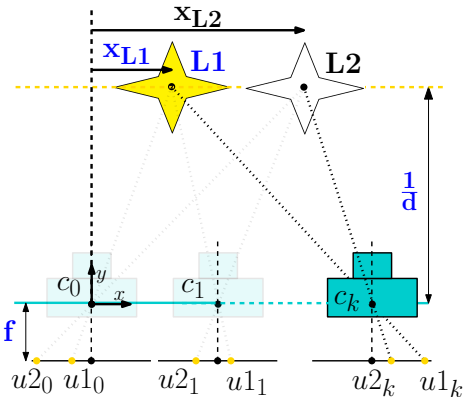

Fig. 2. The monobot performing SLAM with 1 unknown landmark and a beacon. Known quantities are written in blue.

And so the measurement matrix will be

$$H = \begin{bmatrix} -fd & 0 & 0 \\ -fd & 0 & fd \end{bmatrix} \tag{9}$$

And the observability matrix will be given by

$$O = \begin{bmatrix} H \\ HF \\ HF^2 \end{bmatrix} = \begin{bmatrix} -fd & 0 & 0 \\ -fd & 0 & fd \\ -fd & -\Delta t fd & 0 \\ -fd & -\Delta t fd & fd \\ -fd & -2\Delta t fd & 0 \\ -fd & -2\Delta t fd & fd \end{bmatrix} \tag{10}$$

The observability matrix has full rank and hence after inclusion of the beacon, the process is now observable. In fact, it can be shown that the observability matrix will still have full rank for any general number of unknown landmarks, which means that only a single beacon is required for the Monobot to perform SLAM in a one dimensional world with any number of landmarks.

3 Dealing with Beacon Obscurity

We now consider the possibility that after some time, the robot will lose sight of the known landmark and hence the process will reduce to that of the unobservable Case 1. We propose the following measures to ensure observability in such a case

3.1 Procedure

1. We will always treat at least one landmark as the beacon. When the original beacon is obscured, one of the landmarks will be ”beaconized”. Apart from the primary

beacon which is known perfectly, every other secondary beacon will have an associated covariance.

2. Only those landmarks qualify for beaconization whose state covariance has saturated i.e. it cannot be improved further. When the covariance reaches this value, the respective landmark will be excluded from the state and treated as a constant in the measurement equation. The equation will be given as

$$h_{i_{k+1}} = ui_{k+1} - x_{Li} fd = -c_{k+1} fd \tag{11}$$

for the ith landmark. The covariance of x_{Li} will be added to the covariance of ui_{k+1} according to the relation given above to form the overall covariance of the measurement $h_{i_{k+1}}$. Hence the measurement covariance will increase, which is the price we have to pay to maintain observability.

3. Each time a beacon is obscured and a landmark is beaconized, the respective measurement noise covariance will be increased as a function of the covariance of x_{Li}. We will talk about this increase shortly.

3.2 Finding the Steady State Covariance

The first step in the proposed framework would be to find the steady state covariance of the observable landmarks so that we know when the values of their respective covariances are saturated and hence qualify for beaconization. The steady state value of the state covariance can be found beforehand by solving the following discrete algebraic riccatti equation [10]

$$P_\infty = FP_\infty F^T - FP_\infty H^T \left(HP_\infty H^T + R\right)^{-1} HP_\infty F^T + Q \tag{12}$$

where F is the state transition matrix
H is the measurement matrix
R is the measurement noise covariance
Q is the process noise covariance

this value will remain true till R remains constant. When R changes in event of a new beacon, the steady state covariance will then have to be updated. Then from P_∞ we can extract the steady state covariance of the landmark of interest.

3.3 Increasing the Measurement Noise Covariance

Next we need to determine by how much to increase the measurement noise covariance on exclusion of a landmark from the state after its steady state covariance has been achieved. Consider the associated measurement equation before beaconization

$$h_{i_{k+1}} = ui_{k+1} - x_{Li} fd = -c_{k+1} fd \tag{13}$$

when $\sigma^2_{x_{Li}}$ is zero, then $\sigma^2_{h_i} = \sigma^2_{ui}$. This would have been the case if the landmark was perfectly known. For a landmark with an associated covariance, we would have a non zero $\sigma^2_{x_{Li}}$ and can be found out as given in [11] to be

$$\sigma^2_{h_i} = \sigma^2_{ui} + f^2 d^2 \sigma^2_{x_{Li}} + 2fd\mathrm{Cov}(ui, x_{Li}) \tag{14}$$

hence the increase in the measurement noise covariance would be equal to

$$f^2 d^2 \sigma_{x_{Li}}^2 + 2fd\mathrm{Cov}(ui, x_{Li}) \tag{15}$$

3.4 Revisiting a Beacon with Less Covariance

The proposed procedure implies that as more and more landmarks are observed and eventually excluded from the state (after the covariance saturates), the measurement noise covariance will increase continuously. Eventually, a point will be reached when it would not be practical to continue the process, as the measurement noise will affect the lower limit for the state error regardless of the observability.

One possible way to handle this would be to make the robot reobserve a less uncertain beacon every now and then, so as to calibrate itself before the measurement error grows out of bounds. This may be accomplished with an active vision setup. The period after which to reobserve that beacon would be a function of the accuracy of the estimate we require from our application.

We represent the required accuracy as an upper bound on P_∞. This in turn, will specify an upper bound on the covariance matrix of the measurement noise, given by the following rearrangement of Equation 12

$$R = FP_\infty H^T \left(FP_\infty F^T - P_\infty + Q\right)^{-1} HP_\infty F^T - HP_\infty H^T \tag{16}$$

We can use this upper bound on R to determine when it is essential to return to reobserve a relatively certain beacon.

3.5 Simulation

We run simulations for a world containing 1 beacon and 2 landmarks. After a certain point, the beacon is assumed to be obscured from sight of the robot. After this point, we have compared the results of performing beaconization to those of continuing without it. The results are shown in Figures 3 and 4.

We can see that the unbeaconized system diverges. After beaconization, the error of the beaconized landmark in the system of Figure 4 levels off and does not improve. However, the robot continues to successfully track the position and velocity and more notably, the error of the 3rd landmark continues to reduce which is a significant improvement over the system in Figure 3. It should be kept in mind however, that both systems will behave similarly if the initial estimates are fairly exact.

4 Observability for The Monobot in a 2D World

We now extend our analysis for the Monobot to a 2D world where the robot is constrained to move along a single line but the landmarks lie at unknown depth.

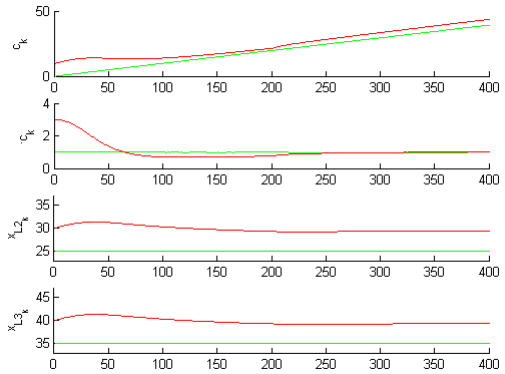

Fig. 3. State evolution without beaconization. The green trajectories represent the true state whereas the red trajectories represent the estimated states. The original beacon is obscured from sight at the 200th interval. From there onwards, the filter can be seen to diverge.

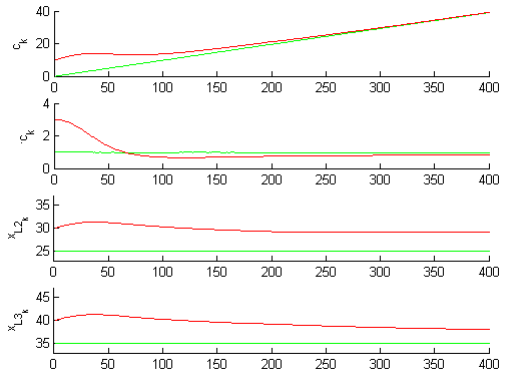

Fig. 4. State evolution with beaconization. After L2 is beaconized, its estimate levels off but the rest of the states continue to converge. A compromise on the convergence of L2 is the price we pay for being able to maintain observability.

4.1 Case 3: A 2D World With 1 Beacon

Robot constrained to move on a single line, observing a beacon and a single landmark with unknown depth, to estimate its own position and the location of the landmark (Figure 5).

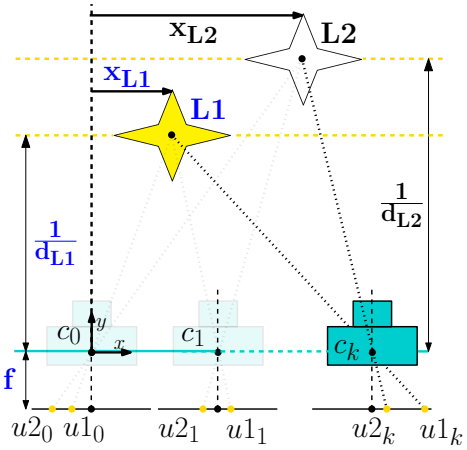

Fig. 5. The monobot performing SLAM in a 2D world with 1 beacon.

The state vector will now be given by

$$X_k = \begin{bmatrix} c_k \\ \dot{c}_k \\ x_{L2_k} \\ d_{L2_k} \end{bmatrix} \tag{17}$$

We now express the process in function form as

$$f = \begin{bmatrix} c_k + \Delta t \dot{c}_k \\ \dot{c}_k \\ x_{L2_k} \\ d_{L2_k} \end{bmatrix} \tag{18}$$

The two measurements are given by

$$\begin{aligned} h_{1_{k+1}} &= u1_{k+1} - x_{L1} f d_{L1} = -c_{k+1} f d_{L1} \\ h_{2_{k+1}} &= u2_{k+1} = x_{L2_{k+1}} f d_{L2_{k+1}} - c_{k+1} f d_{L2_{k+1}} \end{aligned} \tag{19}$$

The measurement equations are non-linear. For the given dimensions of the measurement and state vectors, from [8], the observability matrix in this case will be given by

$$O = \left[d\mathscr{L}_f^1(h_0)\ d\mathscr{L}_f^0(h_2)\ .\ .\ d\mathscr{L}_f^3(h_1)\ d\mathscr{L}_f^3(h_2) \right]^T \tag{20}$$

where $\mathscr{L}_f^n(h_p)$ is the nth order Lie Derivative of the scalar field of the pth measurement with respect to the vector field f and d is the gradient operator. The Observability Matrix turns out to be,

$$O = \left[O_1\ O_2 \right] \tag{21}$$

Where

$$O_1 = \begin{bmatrix} -fd_{L1} & 0 \\ -fd_{L2_k} & 0 \\ -fd_{L1} & -\Delta t f d_{L1} \\ -2fd_{L2_k} & -\Delta t f d_{L2_k} \\ -fd_{L1} & -2\Delta t f d_{L1} \\ -4fd_{L2_k} & -4\Delta t f d_{L2_k} \\ -fd_{L1} & -3\Delta t f d_{L1} \\ -8fd_{L2_k} & -12\Delta t f d_{L2_k} \end{bmatrix} \tag{22}$$

and

$$O_2 = \begin{bmatrix} 0 & 0 \\ fd_{L2_k} & -fc_k + fx_{L2_k} \\ 0 & 0 \\ 2fd_{L2_k} & -2fc_k - \Delta t f\dot{c}_k + 2fx_{L2_k} \\ 0 & 0 \\ 4fd_{L2_k} & -4fc_k - 4\Delta t f\dot{c}_k + 4fx_{L2_k} \\ 0 & 0 \\ 8fd_{L2_k} & -8fc_k - 12\Delta t f\dot{c}_k + 8fx_{L2_k} \end{bmatrix} \tag{23}$$

We can see that O has full rank and so the process is Observable.

4.2 Case 4: Including Disparity as a Measurement

We now see the effect of including disparity as a measurement on Observability. Once more, consider Figure 5. The process and state are the same as given in Equations 17 and 18. But we now have three non-linear measurements. The first 2 are given by Equation 19, and the third one being disparity, given as

$$h_{3_k} = u2_k - u2_{k-1} = -fc_k d_{L2_k} + fc_{k-1} d_{L2_k} \tag{24}$$

The Observability Matrix comes out to be full rank for the world shown in Figure 5. It is interesting to see what happens if we exclude the beacon so that we are now performing SLAM with only a single landmark. In this case, the Observability Matrix turns out to be

$$O = \begin{bmatrix} O_1 & O_2 \end{bmatrix} \tag{25}$$

Where

$$O_1 = \begin{bmatrix} -fd_{L2_k} & 0 \\ -fd_{L2_k} & 0 \\ -2fd_{L2_k} & -\Delta t f d_{L2_k} \\ -2fd_{L2_k} & -\Delta t f d_{L2_k} \\ -4fd_{L2_k} & -4\Delta t f d_{L2_k} \\ -4fd_{L2_k} & -4\Delta t f d_{L2_k} \\ -8fd_{L2_k} & -12\Delta t f d_{L2_k} \\ -8fd_{L2_k} & -12\Delta t f d_{L2_k} v \end{bmatrix} \tag{26}$$

and

$$O_2 = \begin{bmatrix} fd_{L2_k} & -fc_k + fx_{L2_k} \\ 0 & -fc_k + fc_{k-1} \\ 2fd_{L2_k} & -2fc_k - \Delta t f\dot{c}_k + 2fx_{L2_k} \\ 0 & -2fc_k - \Delta t f\dot{c}_k + fc_{k-1} \\ 4fd_{L2_k} & -4fc_k - 4\Delta t f\dot{c}_k + 4fx_{L2_k} \\ 0 & -4fc_k - 4\Delta t f\dot{c}_k + fc_{k-1} \\ 8fd_{L2_k} & -8fc_k - 12\Delta t f\dot{c}_k + 8fx_{L2_k} \\ 0 & -8fc_k - 12\Delta t f\dot{c}_k + fc_{k-1} \end{bmatrix} \tag{27}$$

which is still full rank. This suggests that including disparity as a measurement may have eliminated the need for the beacon.This also formalizes the need for triangulation as done by including multiple time segments in [2].

4.3 Simulation

In this section we simulate the Kalman filter for Case 4 both with and without disparity as a separate measurement. We have assumed a world with the robot performing SLAM with a single landmark. As does theory, simulations show that observability can be acheived in the unobservable case of a single landmark world by measuring disparity separately. The results can be seen in Figure 6.

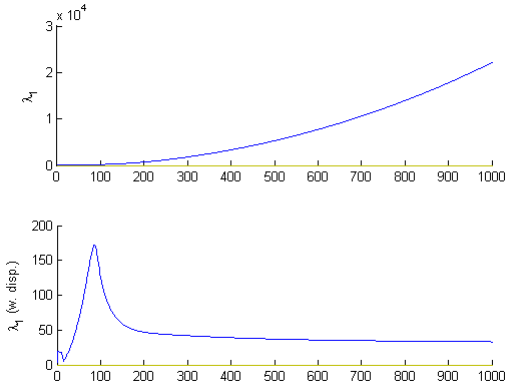

Fig. 6. Results of measuring disparity separately. The top plot is the first eigenvalue of the covariance matrix of a system without measuring disparity. It can be seen that the covariance blows up. The bottom plot represents a system which measures disparity. The plotted eigenvalue along with all others not shown here are bounded, which demonstrates observability.

5 The Kalman filter with disparity as a separate measurement

Including disparity into the Kalman filter as a measurement in monocular SLAM is unconventional because in our case disparity is a measurement dependent on the current and previous states whereas the Kalman filter assumes that the measurement is dependent on the current state only. We derive the Kalman filter for this case from the basic Bayes filter following the method given in [12]. We first present the equations and then follow with the complete proof.

Prediction:

$$\hat{X}_{k|k-1} = f(\hat{X}_{k-1|k-1}, \mu_k, 0) \tag{28}$$

$$P_{k|k-1} = F_{X_{k-1}} P_{k-1|k-1} {F_{X_{k-1}}}^T + F_{\omega_k} Q_k {F_{\omega_k}}^T \tag{29}$$

Measurement Covariance:

$$W_k = R_k + H_{X_{k-1}} G_{\omega_k} Q_k {G_{\omega_k}}^T {H_{X_{k-1}}}^T \tag{30}$$

Kalman Gain:

$$K_k = P_{k|k-1} {H_{X_k}}^T (H_{X_k} P_{k|k-1} {H_{X_k}}^T + W_k)^{-1} \tag{31}$$

Correction:

$$\hat{X}_{k|k} = \hat{X}_{k|k-1} + K_k(Y_k - h(\hat{X}_{k|k-1}, \hat{X}_{k-1|k-1})) \tag{32}$$

$$P_{k|k} = (I - K_k H_{X_k}) P_{k|k-1} \tag{33}$$

where

$\hat{X}_k$	- The estimate of X at time step k
P_k	- The covariance of $\hat{X}_k$
μ_k	- The control vector at time step k
$\hat{Y}_k$	- The expected measurement at time step k
K_k	- The Kalman gain matrix at time step k
W_k	- The covariance of $\hat{Y}_k$
$f(X_{k-1}, \mu_{k-1})$	- The motion model
$g(X_k, \mu_k)$	- The inverse motion model
$h(X_k, X_{k-1})$	- The measurement model

The difference between the EKF equations for simple measurement models (not dependent on the previous state) and this one lies in the calculation in Equation 30. For simple measurement models, W_k would just have been equal to the sensor noise R_k. And the rest of the equations would have remained unchanged. Note that for linear systems, the inverse motion model will just be equal to F^{-1}. We assume that such an inversion exists.

The proof of the modified EKF equations is given as follows

Functions and variables

Motion Model The motion or process model is given by

$$X_k = f(X_{k-1}, \mu_k, \omega_k)$$

Where ω_k is the process noise at step k. Its covariance is given by Q_k. After linearization we get the following form

$$X_k = f(\hat{X}_{k-1}, \mu_k, 0) + F_{X_{k-1}}(X_{k-1} - \hat{X}_{k-1}) + F_{\omega_k}\omega_k$$

Where
$F_{X_{k-1}}$ - is the Jacobian of f w.r.t X_{k-1}
F_{ω_k} - is the Jacobian of f w.r.t ω_k

Inverse Motion Model The inverse motion model is given by

$$X_{k-1} = g(X_k, \mu_k, \omega_k)$$

Note that for same time steps, ω_k has the same value as its instance appearing in the motion model. After linearization we get

$$X_{k-1} = g(\hat{X}_k, \mu_k, 0) + G_{X_k}(X_k - \hat{X}_k) + G_{\omega_k}\omega_k$$

Where
G_{X_k} - is the Jacobian of g w.r.t X_k
G_{ω_k} - is the Jacobian of g w.r.t ω_k

Measurement Model The measurement model is given by

$$Y_k = h(X_k, X_{k-1}) + v_k$$

Where v_k is the sensor noise. Its covariance is given by R_k. After linearization we get

$$\begin{aligned} Y_k =& h(\hat{X}_k, \hat{X}_{k-1}) + H_{X_k}(X_k - \hat{X}_k) \\ &+ H_{X_{k-1}}(X_{k-1} - \hat{X}_{k-1}) + v_k \end{aligned} \tag{34}$$

Where
H_{X_k} - is the Jacobian of h w.r.t X_k
$H_{X_{k-1}}$ - is the Jacobian of h w.r.t X_{k-1}

Mathematical Derivation

The equations are derived first by extending the basic Bayes Filter Algorithm, to include the previous state in the measurement step. Then the probability distributions are solved for the required models. To include the dependency of Y_k on X_{k-1} we include an intermediate step in the Bayes Filter through the theorem of total probability. The steps are as follows

Step 1

$$\begin{aligned} \overline{bel(X_k)} &= p(X_k | Y_{0:k-1}, \mu_k) \\ &= \int p(X_k | X_{k-1}, Y_{0:k-1}, \mu_k) p(X_{k-1} | Y_{0:k-1}, \mu_k) \mathrm{d}X_{k-1} \end{aligned} \tag{35}$$

Step 2

$$p(Y_k|X_k, Y_{0:k-1}, \mu_k) = \int p(Y_k|X_k, Y_{0:k-1}, \mu_k, X_{k-1}) p(X_{k-1}|X_k, Y_{0:k-1}, \mu_k) \mathrm{d}X_{k-1} \tag{36}$$

Step 3:

$$bel(X_k) = \eta\, p(Y_k|X_k, Y_{0:k-1}, \mu_k) p(X_k|Y_{0:k-1}, \mu_k) \tag{37}$$

We present the derivation, with this extended form of the Bayes filter

Part 1: Prediction We begin with step 1 of the Bayes filter. The terms of Equation (35) are normally distributed with mean and covariance as

$$\underbrace{p(X_k|X_{k-1}, Y_{0:k-1}, \mu_k)}_{N\sim(X_k; f(\hat{X}_{k-1}, \mu_k, 0) + F_{X_{k-1}}(X_{k-1} - \hat{X}_{k-1}); F_{\omega_k} Q_k {F_{\omega_k}}^T)}$$

and

$$\underbrace{p(X_{k-1}|Y_{0:k-1}, \mu_k)}_{N\sim(X_{k-1}; \hat{X}_{k-1}; P_{k-1})}$$

After evaluation of this equation, the outcome is also a Gaussian with mean $\hat{X}_{k|k-1}$ and covariance $P_{k|k-1}$. The interested reader is directed to [12] for the full proof. Here we present the equations. The mean and variance of the resulting distribution are given as

$$\hat{X}_{k|k-1} = f(X_{k-1}, \mu_k, 0) \tag{38}$$

$$P_{k|k-1} = (F_{\omega_k} Q_k {F_{\omega_k}}^T) + F_{X_{k-1}} P_{k-1} {F_{X_{k-1}}}^T \tag{39}$$

Part 2: Measurement Covariance Step 2 of the extended Bayes filter given by (36). The distributions of the terms involved are given as follows

$$\underbrace{p(Y_k|X_k, Y_{0:k-1}, \mu_k, X_{k-1})}_{(\sim N(Y_K; h(\hat{X}_k, \hat{X}_{k-1}) + H_{x_k}(X_k - \hat{X}_k) + H_{X_{k-1}}(X_{k-1} - \hat{X}_{k-1}); R_k))}$$

$$\underbrace{p(X_{k-1}|X_k, Y_{0:k-1}, \mu_k)}_{(\sim N(X_{k-1}; g(\hat{x}_k, \mu_k, 0) + G_{X_k}(X_k - \hat{X}_k); G_{\omega_k} Q_k {G_{\omega_k}}^T))}$$

The derivation is essentially the same as that of step 1 given in [12]. In this case the integral in Equation 36 can be expressed as

$$\int \exp\{-M_k\} \mathrm{d}X_{k-1} \tag{40}$$

Where

$$\begin{aligned} M_k = & \frac{1}{2}\Big(Y_k - h(\hat{X}_k,\hat{X}_{k-1}) - H_{x_k}(X_k-\hat{X}_k) - H_{X_{k-1}}(X_{k-1}-\hat{X}_{k-1})\Big)^T \\ & {R_k}^{-1}\Big(Y_k - h(\hat{X}_k,\hat{X}_{k-1}) - H_{x_k}(X_k-\hat{X}_k) - H_{X_{k-1}}(X_{k-1}-\hat{X}_{k-1})\Big) \\ & + \frac{1}{2}\Big(X_{k-1} - g(\hat{x}_k,\mu_k,0) - G_{X_k}(X_k-\hat{X}_k)\Big)^T \Big(G_{\omega_k} Q_k {G_{\omega_k}}^T\Big)^{-1} \\ & \Big(X_{k-1} - g(\hat{x}_k,\mu_k,0) - G_{X_k}(X_k-\hat{X}_k)\Big) \end{aligned} \tag{41}$$

We can decompose M_k into two functions. These functions are given by

$$M_k = M(Y_k, X_k, X_{k-1}) + M(Y_k, X_k) \tag{42}$$

By differenciating twice with respect to X_{k-1}, we determine the minimum and covariance of M_k so as to form a quadratic function similar to the exponential of the normal distribution. Thus we get

$$\begin{aligned} & M(Y_k, X_k, X_{k-1}) \\ = & \frac{1}{2}\Big(X_{k-1} - \Phi_k\Big({H_{X_{k-1}}}^T {R_k}^{-1}(Y_k - h(\hat{X}_k,\hat{X}_{k-1}) - H_{x_k}(X_k-\hat{X}_k) \\ & - H_{X_{k-1}}(X_{k-1}-\hat{X}_{k-1})) \\ & + (G_{\omega_k} Q_k {G_{\omega_k}}^T)^{-1}(g(\hat{x}_k,\mu_k,0) - G_{X_k}(X_k-\hat{X}_k))\Big)\Big)^T \Phi_k^{-1} \\ & \Big(X_{k-1} - \Phi_k\Big({H_{X_{k-1}}}^T {R_k}^{-1}(Y_k - h(\hat{X}_k,\hat{X}_{k-1}) - H_{x_k}(X_k-\hat{X}_k) \\ & - H_{X_{k-1}}(X_{k-1}-\hat{X}_{k-1})) \\ & + (G_{\omega_k} Q_k {G_{\omega_k}}^T)^{-1}(g(\hat{x}_k,\mu_k,0) - G_{X_k}(X_k-\hat{X}_k))\Big)\Big) \end{aligned} \tag{43}$$

Where

$$\Phi_k = \Big({H_{X_{k-1}}}^T {R_k}^{-1} H_{X_{k-1}} + (G_{\omega_k} Q_k {G_{\omega_k}}^T)^{-1}\Big)^{-1} \tag{44}$$

Hence from (41), (42) and (43), we get $M(Y_k, X_k)$. As this does not have any dependence on X_{k-1}, we can move it out of the integral. What remains inside the integral is $exp\{-M(Y_k, X_k, X_{k-1}\}$ which is a valid probability density function hence integrates to a constant. Thus $exp\{-M(Y_k, X_k\}$ gives the required distribution. The mean and covariance of this distribution is given by the minimumm and inverse of the curvature of $M(Y_k, X_k)$ respectively. Differenciating with respect to Y_k, we get the mean as

$$h(\hat{X}_k, \hat{X}_{k-1}) + H_{X_k}(X_k - \hat{X}_k) \tag{45}$$

And the covariance, the inverse of the curvature, given as

$$W_k = R_k + H_{X_{k-1}} G_{\omega_k} Q_k {G_{\omega_k}}^T {H_{X_{k-1}}}^T \tag{46}$$

This proves the correctness of (30).

Part3: Correction / Update The distributions of the terms involved in the 3rd step of the Bayes Filter are

$$\underbrace{p(Y_k|X_k, Y_{0:k-1}, \mu_k)}_{\left(\sim N(Y_k; h(\hat{X}_k, \hat{X}_{k-1}) + H_{X_{k-1}}(X_k - \hat{X}_k))\right)}$$

$$\underbrace{p(X_k|Y_{0:k-1}, \mu_k)}_{\left(\sim N(X_k; f(\hat{X}_{k-1}, \mu_k, 0); F_{X_{k-1}} P_{k-1} {F_{X_{k-1}}}^T + F_{\omega_k} Q_k {F_{\omega_k}}^T)\right)}$$

The resulting distribution follows from [12] by replacing R_k with W_k so that we get the remaining equations.

$$\hat{X}_{k|k} = \hat{X}_{k|k-1} + K_k\left(Y_k - h(\hat{X}_k, \hat{X}_{k-1})\right) \tag{47}$$

$$K_k = P_{k|k-1} {H_{X_k}}^T (H_{X_k} P_{k|k-1} {H_{X_k}}^T + W_k)^{-1} \tag{48}$$

$$P_{k|k} = (I - K_k H_{X_k}) P_{k|k-1} \tag{49}$$

6 Extension to general 2D SLAM

From this point forth, the calculations for obtaining the nonlinear observability matrices become highly complex. As of yet, the calculations are unable to be carried out even by a computer algebraic package. It may be possible to prove the rank criterion through mathematical induction, as done in [13]. Simulations for this case have been done in [2]. Here, we present a geometrical argument to extend the analysis to 2 dimensions.

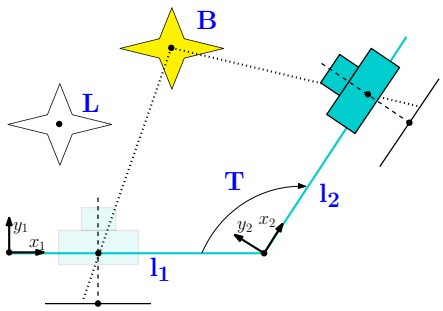

Fig. 7. Robot moving first along line l_1 then along l_2. A landmark L and a beacon B are being measured. The transformation between the lines is given by T

Till now we have proved that a robot executing linear motion in a 2D world is able to perform SLAM. Now consider Figure 7. Without any beacon, the robot will be able to determine SLAM coordinates within each frame attached to l_1 and l_2. But it does not know the transformation T between the lines which does not allow for full absolute

coordinate SLAM. It can be shown that this transformation may be calculated with only 1 beacon through triangulation. This reconciles with the work done in [2] in which it is also deduced that 1 beacon is sufficient to perform monocular SLAM in 2D.

7 Conclusion

The observability analysis performed in this paper apart from reconciling the results acheived from linear observability analysis, has made two major contributions. Firstly, it has enabled us to provide a strategy for maintaining filter stability in the event of beacon obscurity. Although the strategy has been presented for 1 dimensional SLAM, it is easily extended to further dimensions. Moreover, this strategy applies not only to monocular SLAM but also to SLAM in general where the shortage of beacons may be an issue. Secondly, we have used this analysis to fromalize the need for triangulation in a different way than has been done in related literature. We have shown that inclusion of disparity as a measurement in the filter improves performance and have also calculated the ammendments in the Kalman filter required for this purpose. These are important results and should allow the design of more accurate observers.

References

1. P. Bonnifait and G. Garcia, "Design and experimental validation of an odometric and goniometric localization system for outdoor robot vehicles," *Robotics and Automation, IEEE Transactions on*, vol. 14, no. 4, pp. 541–548, 1998.
2. T. Vidal-Calleja, M. Bryson, S. Sukkarieh, A. Sanfeliu, and J. Andrade-Cetto, "On the observability of bearing-only slam," in *Robotics and Automation, 2007 IEEE International Conference on*. IEEE, 2007, pp. 4114–4119.
3. J. Kim and S. Sukkarieh, "Improving the real-time efficiency of inertial slam and understanding its observability," in *Intelligent Robots and Systems, 2004.(IROS 2004). Proceedings. 2004 IEEE/RSJ International Conference on*, vol. 1. IEEE, 2004, pp. 21–26.
4. D. Goshen-Meskin and I. Bar-Itzhack, "Observability analysis of piece-wise constant systems. i. theory," *Aerospace and Electronic Systems, IEEE Transactions on*, vol. 28, no. 4, pp. 1056–1067, 1992.
5. M. Tribou, D. Wang, and W. Wilson, "Observability of planar combined relative pose and target model estimation using monocular vision," in *American Control Conference (ACC), 2010*. IEEE, 2010, pp. 4546–4551.
6. T. Manzoor, A. Munawar, and A. Muhammad, "Visual servoing of a sensor arm for mine detection robot marwa," *ROBOTIK 2012*, 2012.
7. A. Davison, "Real-time simultaneous localisation and mapping with a single camera," in *Computer Vision, 2003. Proceedings. Ninth IEEE International Conference on*. Ieee, 2003, pp. 1403–1410.
8. R. Hermann and A. Krener, "Nonlinear controllability and observability," *Automatic Control, IEEE Transactions on*, vol. 22, no. 5, pp. 728–740, 1977.
9. K. Ogata, *Modern control engineering*. Prentice Hall PTR, 2001.
10. D. Simon, *Optimal state estimation: Kalman, H [infinity] and nonlinear approaches*. John Wiley and Sons, 2006.
11. D. Montgomery and G. Runger, *Applied statistics and probability for engineers*. Wiley, 2010.

12. D. Fox, S. Thrun, and W. Burgard, *Probabilistic robotics*. the MIT Press, 2005.
13. L. Perera, A. Melkumyan, and E. Nettleton, "On the linear and nonlinear observability analysis of the slam problem," in *Mechatronics, 2009. ICM 2009. IEEE International Conference on*. Ieee, 2009, pp. 1–6.